

See discussions, stats, and author profiles for this publication at: <https://www.researchgate.net/publication/325529314>

# Micro-manufacturing Technology Using DUV Laser and NC\*

Article in *Advances in Systems Science and Applications* · January 2011

CITATIONS

0

READS

49

3 authors, including:



Jianlei Cui

Xi'an Jiaotong University

68 PUBLICATIONS 894 CITATIONS

SEE PROFILE

Some of the authors of this publication are also working on these related projects:



nanofabrication by AFM probe tip [View project](#)



nanostructure fabrication by AFM tip [View project](#)

## Micro-manufacturing Technology Using DUV Laser and NC\*

Gang Xu, Yutang Dai and Jianlei Cui

Key Laboratory of Fiber Optic Sensing Technology, Wuhan University of Technology,  
Wuhan 430070, China

**Abstract** Combining deep UV laser with NC technology, complex 3D structures can be generated. For fused silica, the ablation depth and surface roughness are investigated after 157nm laser processing. Under laser fluence of  $\sim 4\text{J}/\text{cm}^2$  and spot size of  $\sim 35\mu\text{m}$ , the ablation rate of fused silica is about 75nm/pulse for 157nm laser. A better ablation quality could be achieved under the repetition rate of  $\sim 10\text{Hz}$ . Assisted by numerical control, three-dimensional micro-structures are fabricated using 157nm laser technique.

**Keywords** DUV laser, Micro-manufacturing, Numerical control, Fused silica

### 1.Introduction

MOEMS (Micro-Optical-Electro-Mechanical System) is a very dynamic research direction developed from MEMS technology in recent years, which is a new type of micro-optical system resulting from the combination of micro-mechanical, micro-electronics and micro-optics. MOEMS device has smaller size, lighter weight, so has lower power consumption, smaller inertia, shorter response times, etc<sup>[1,2,3,4]</sup>. But the forecast advantages are not fully reflected, in large part due to the poor level of micro-mechanical processing<sup>[5]</sup>. Currently, the majority of such photonics chips or MEMS parts are planar devices based on silicon or silica-on-silicon substrates but the manufacturing procedures are still largely reliant on combinations of conventional exposure and etching steps. In particular, three-dimensional structuring of most MEMS parts is usually reliant on LIGA process<sup>[6]</sup>. There are so many constraints using abovementioned process that developments of more cost-effective process is needed. Among various new manufacturing methods, laser micro-processing is a promising choice. One of the main attractions of laser micro-processing is that lasers offer great flexibility in the rapid prototyping and evaluation of different designs. Many different process routes can also be tried out with the same laser tool in a relatively short time so the developmental cycle is also much faster than with many conventional techniques.

$\text{SiO}_2$  has low thermal expansion coefficient, permeability to gases and to ionic contaminants, excellent chemical inertness, good electric insulation, and has more attractive mechanical properties than ordinary glass<sup>[7,8,9]</sup>, it has become one of the most important materials for fabricating Optical lens and MOEMS devices, such as micro fluidic chip, SOC (system on chip) and MCM(multi-chip module). However, fused silica is relatively transparent for visible light and ultraviolet radiation, which can not be effectively absorbed, so the issue of how to process it efficiently is of crucial importance. Due to development of special optical component, three dimension micromachining with deep-ultraviolet laser (DUV, mainly 157nm laser) has become feasible technically. The photon energy of 157 nm laser is up to 7.9-eV<sup>[10]</sup>, can directly hit the ionic bond of  $\text{SiO}_2$  by photo-chemical effect. Besides, 157nm laser have the benefit of being compatible with mask projection systems, so that a precision laser-ablation processing can be performed on glass surfaces. The main process steps of laser direct ablation with the sample are shown in Fig. 1.

---

\* National Natural Science Foundation of China (Grant No.50775169 and No.60537050)

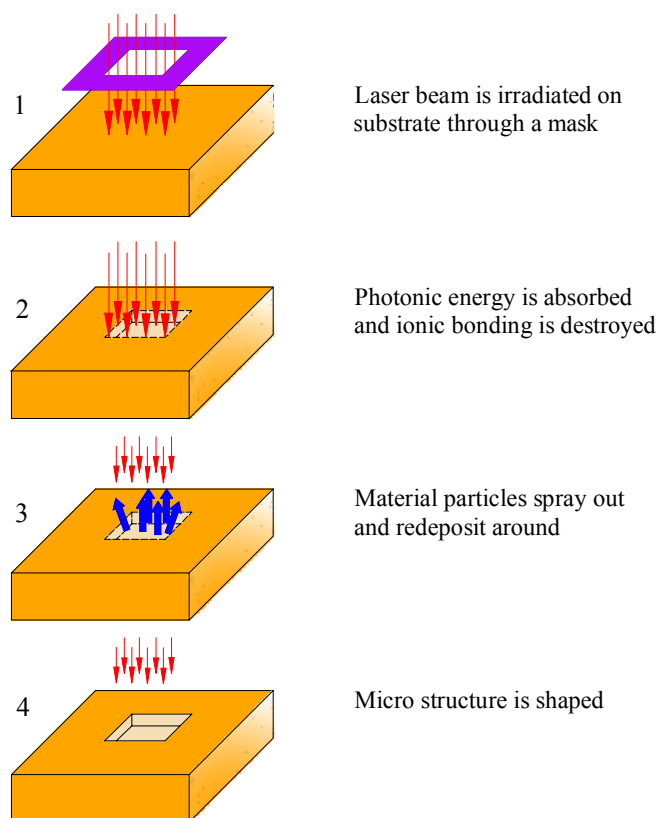


Fig.1. The ablation steps of 157nm laser process

In this study, preliminary research on micro-ablation of 157nm DUV laser was performed. The main aim of those researches is to investigate the micro-processing performance of 157nm laser. Influence of laser process parameters on surface quality was investigated. 3D micro-structures produced by DUV laser and NC process, are demonstrated.

## 2.DUV Laser Micromachining System

A dual-laser system (M2000: Dual Laser Processing Tool) manufactured by Exitech Ltd of England was used. The system is adaptive to wide variety of laser processing requirements, based around UV laser materials processing. Two laser sources are fitted to the M2000. In one case the beam from a high repetition rate UV DPSS laser operating at 355nm illuminates an aperture. This is then imaged onto the workpiece using a high resolution projection lens. In the other case an F<sub>2</sub> laser is fitted which operates at a wavelength of 157nm. The beam from this is imaged onto the workpiece using a high resolution reflective lens. Fig. 2 illustrates Schematic of dual-laser precision micro-ablation system. The 157nm laser source is the Model M-100 manufactured by Tui Laser of Germany. The pulse duration is 20ns, and the pulse repetition rate is 100Hz. The output of the 157nm laser source is 1.5W, and the laser pulse energy is 25mJ. Due to the high absorption of 157nm radiation in the atmosphere, - at atmospheric pressure the photon penetration of O<sub>2</sub> is only ~50μm, the entire beam path from the laser output coupler to the sample was purged with high purity nitrogen. The purge gas escaped from the bottom of the Schwarzschild lens onto the sample. The purging also helps prevent contamination of the optics by deposited films from airborne organic contaminants that are photo-dissociated by 157nm radiation.

The workpiece mounted on the worktable can be moved by 4-axis (X, Y, Z and R) NC stages. Motions of the stages and the firing of the laser are coordinated by the Aerotech Unidex 500 Motion Controller. Providing up to four axes of synchronized servo control and four axes of stepper control, the Unidex 500 supports the motion requirements of today's most demanding machines. The parameters of the motion control stages are shown in Table 1, and Fig. 3 shows the schematic of the motion system.

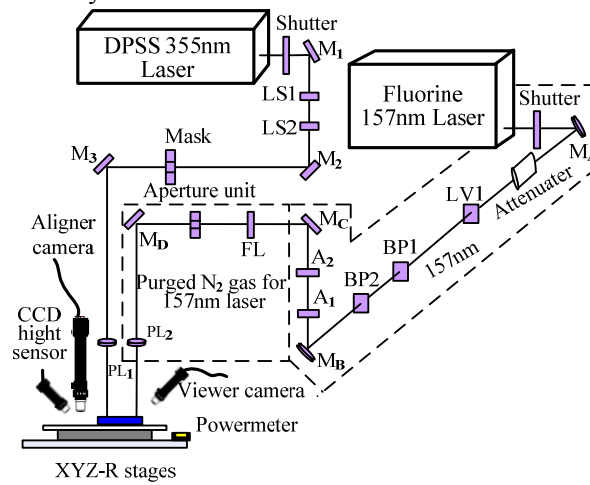


Fig.2. Schematic of optical system of dual laser process tool

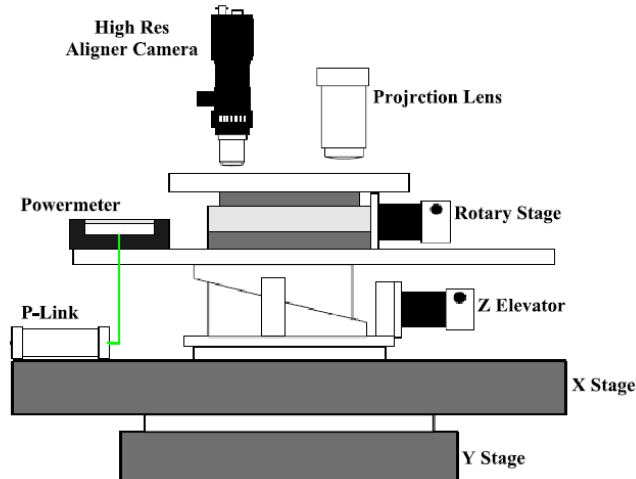


Fig.3. Schematic of the motion control stages

Table 1 The parameters of the Aerotech motion control stages

Axis	Description	Travel	Drive	Resolution	Maximum feedrate	Typical feedrate
X	X workpiece	300mm	AC linear motor	0.5um	60000mm/min	10000mm/min
Y	Y workpiece	300mm	AC linear motor	0.5um	60000mm/min	10000mm/min
Z	Focus	10mm	AC brushless motor	0.1um	500mm/min	250mm/min
R	Workpiece rotation	$\pm 45^\circ$	AC brushless motor	0.8mdeg	5rpm	1rpm
A	Attenuator	0-1	Stepper motor	0.01	1/sec	0.25/sec

### 3.Laser Micro-Ablation Experiments

#### 3.1 Ablation rates

Fig. 4 shows VUV–UV transmission spectra of fused silica at room temperature. Fused silica is relatively transparent when laser wavelength is larger than 180nm. But the transparency decrease dramatically as the wavelength is lower than 175nm. This means that 157nm laser beam can be better absorbed by fused silica.

Not only is the range of materials which can be machined enlarged by using 157nm radiation, but the higher machining quality can be achieved. In general, the ablation rate is largely affected by absorption coefficients  $\alpha$  of materials and laser fluences  $F$ . In the 157nm laser ablation, the material removal is predominantly photon-chemical process.

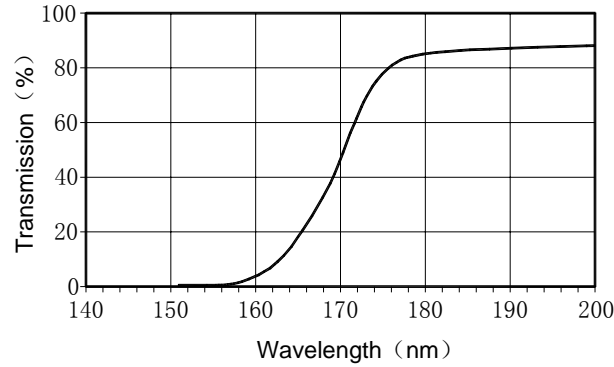


Fig.4. UV transmission of fused silica

For incident laser fluences just above an ablative threshold value  $F_T$ , the etch depth per pulse  $t$  is approximately:

$$t = \frac{1}{\alpha} \ln \left[ \frac{F}{F_T} \right] \quad (1)$$

For a laser pulse duration  $\tau$  giving a temperature rise  $\Delta T$  to the vaporization point of a material with density  $\rho$ , specific heat  $C_p$  and reflectivity  $R$  of the surface at the laser wavelength, the ablation threshold is given by:

$$F_T = \frac{1}{\alpha} \frac{\Delta T \rho C_p}{(1 - R)} \quad (2)$$

For photon absorption, the penetration depth of  $1/\alpha$  is dependent on laser wavelength, bandgap energy of materials and so on. The higher the photon absorption, the smaller the ablation threshold and etch depth per pulse (Eqs. 1 and 2). As for fused silica ablated by 157nm laser, the penetration depth is about 59nm, and the ablation threshold of  $F_T$  is about 1.0J/cm<sup>2</sup>. Through calculation, the ablation depth is about 81nm per pulse as fluence of 157nm laser was 4J/cm<sup>2</sup>. In this study, we also measured laser ablation depth under conditions with different laser pulses and constant energy ( $F=4\text{J/cm}^2$ ), as shown in Fig. 5. The 157nm laser spot size was about 35 $\mu\text{m} \times 35\mu\text{m}$ . As the number of pulses is smaller than 100, the ablation rates is 73-77nm per pulse, generally close to the calculation result. But the ablation rate reduces gradually to about 50nm per pulse as the number of pulses increase to 600<sup>[11]</sup>. That is result from energy reduction when the ablated material far from the focusing plane, even though the energy is still constant on the focusing plane.

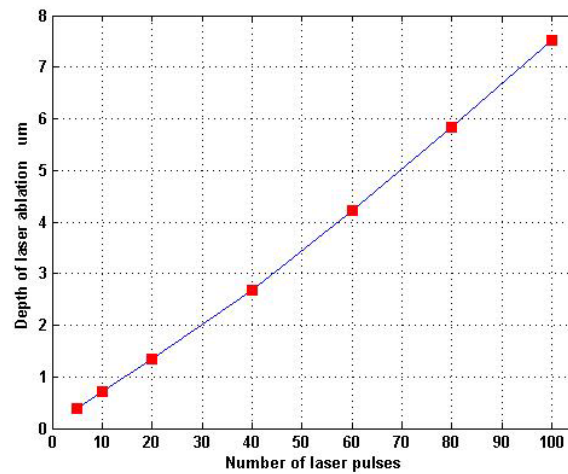
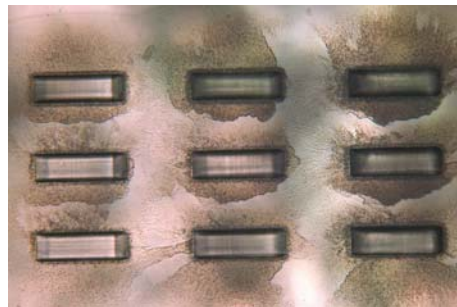


Fig.5. Relationship between ablation depth and number of laser pulses ( $F=4\text{J}/\text{cm}^2$ )

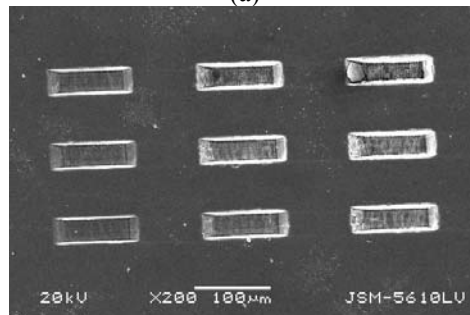
### 3.2 Micromachining of Silica Glasses

157nm laser beam can be largely absorbed ( $\alpha=170,000\text{ cm}^{-1}$ ) by fused silica, it can thus be used for 3D micro-structuring tool for silica materials. Fig. 6 shows channels formed by a  $20\mu\text{m}\times 20\mu\text{m}$   $F_2$  laser beam scanning along the horizontal direction in fused silica. The size of each channel is  $\sim 120\mu\text{m}\times 20\mu\text{m}$ . The ablating conditions are: repetition rate for each column is 8Hz, 12Hz and 16Hz, respectively; scanning velocity for each row is 0.18mm/min, 0.23mm/min and 0.28mm/min, respectively; laser fluence is  $\sim 4\text{J}/\text{cm}^2$ , the scanning cycles are three loops.

The plume dynamics in laser ablation of silica glasses generates non-volatile products, so after ablation, some of re-deposited particles scattered onto and over nearby the ablated surface, as shown in Fig. 6(a).



(a)



(b)

Fig.6. The images of the channels ablated on silica glasses using 157nm laser (a) ablation debris deposited around the channels, immediately after ablation (b) the SEM image after ultrasonic cleaning in HF solution

Submicron order glass particulates will collect and partially sinter on surfaces to form coatings around small structures, and growing thicker and broader with the volume of material removed by the laser. Since there is no strong bonding between the re-deposited particles, the debris tends to be rather weak in structure and can be easily removed by etching process using vol. <10% HF acid. The SEM image shown in Fig. 6(b) is the result after 5 minutes ultrasonic cleaning in 5% HF solution. It is seen that, the channels produced by 157nm laser is relatively regular and precise.

Using a profiler, the depth of each channels were measured. Fig. 7 shows the depth of the channels under different ablating conditions. The measured results is very close to the theoretical value. The depth of the channel can be calculated by:

$$h = \frac{L \cdot f \cdot t \cdot n}{v} \quad (3)$$

L: Length of laser spot along scanning direction

v: Shift velocity of the workpiece

f: Pulse repetition frequency

t: Etch depth per pulse

n: Scanning loops

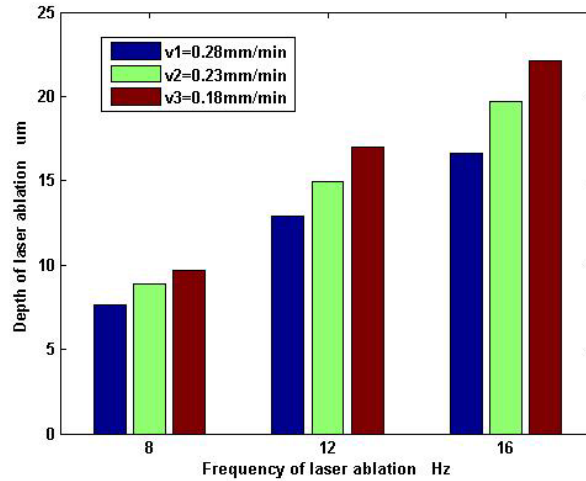


Fig.7. The depth of the channels under different frequency and velocity

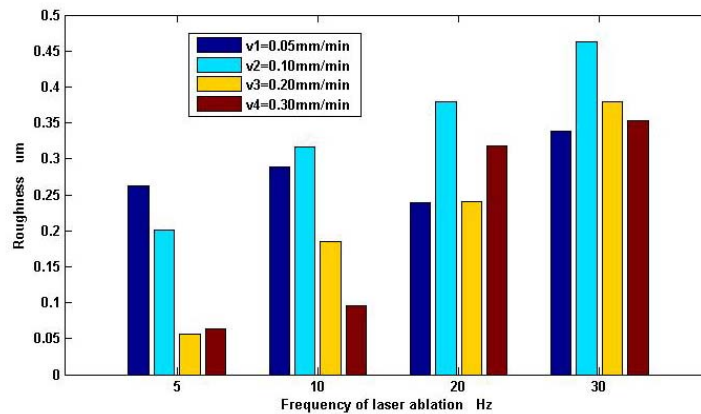


Fig.8. The relationship between roughness and laser parameters (frequency, velocity)

We also investigated ablated surface roughness of fused silica under different process parameters. Like shown in Fig. 6, the short channels ( $4 \times 4$  array) were produced using a quadrate beam, the spot size  $\sim 35\mu\text{m} \times 25\mu\text{m}$ , the laser fluence  $\sim 4\text{J}/\text{cm}^2$ . We changed laser pulse repetition rate from 5Hz to 30Hz, and the shift velocity of worktable from 0.05mm/min to 0.30mm/min. Fig. 8 shows the ablated bottom roughness  $R_a$  of channels for the different scanning velocity and repetition rate. It is obvious that, there exists a strong dependence of the surface quality on the laser process parameters. On the whole, when laser repetition rate increases, the averaged roughness of the channel bottom would become larger, i.e. the surface quality become worse. And, slower laser scanning velocity such as  $v=0.05\text{mm}/\text{min}$  is not recommended, because the averaged roughness shows higher value. Using high velocity ( $v=0.2\text{ mm}/\text{min}$  or  $0.30\text{mm}/\text{min}$ ) and low pulse repetition rate ( $f=5\text{Hz}$ ), the ablated surface roughness is very low. But take into account the machining efficiency, the repetition rate of 10Hz is better. From the trend of ablated roughness, the influence of the heat produced during the laser process and the cleaning process with HF solution can not be ignored. In fact, when the laser ablation was performed under higher repetition rate and lower scanning speed, the accumulation of heat become bigger at same point, so that thermo-stress would formed at bottom of the channel. After ultrasonic cleaning with HF solution, cracks resulting from the thermo-stress would be produced, like the upper-right channel shown in Fig. 6. This causes the increase of bottom roughness.

### 3.3 Micromachining assisted by Numerical Control

NC programming is an important part of laser processing, which affects the processing quality and production efficiency<sup>[12]</sup>. In this paper, the NC programming system is AlphaCAM which programmed by Licom system Ltd of England. Based upon geometric graphics information, this system can automatically generate and optimize the tool-path. As the user input the process parameters on the basis of the tool-path, the system then generate laser processing NC code automatically, includes the laser fire on/off control. The flow chart of laser micro-manufacturing is shown in Fig. 9. Trajectory optimization is aimed at generating the reasonable laser processing tool-path, getting the shortest processing path and the least number of laser switching, and then improving the efficiency of laser processing. Typically, the processing parameters include laser fluence, beam size, pulse repetition frequency, scanning velocity (for processing with scanning mode) and total pulse numbers (usually for machining at a constant position).

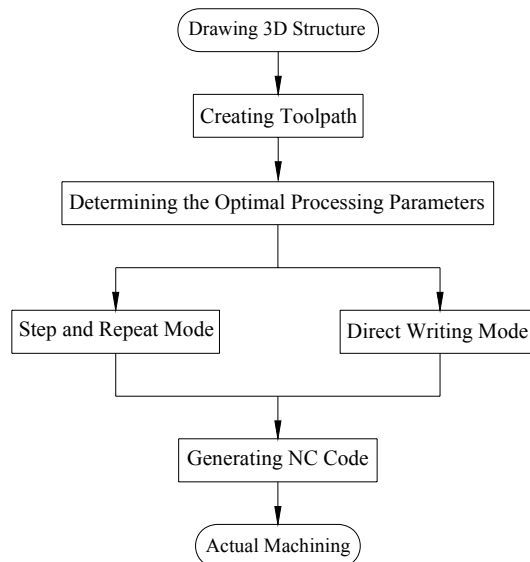
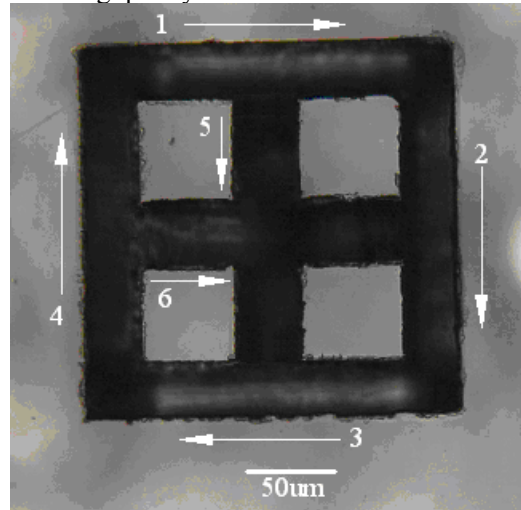


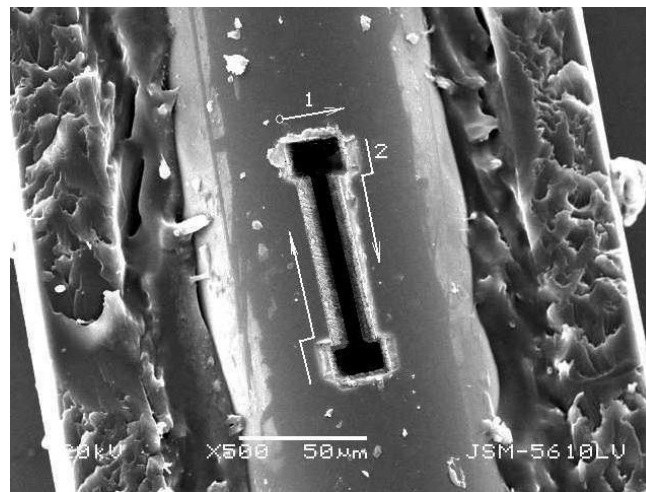
Fig.9. The flow chart of laser processing



As examples of laser NC micromachining, Fig. 10 shows two microstructures fabricated by 157nm laser. Fig. 10(a) is a Chinese character “田”. The process tool-path was decided as from line 1 to line 6. The process parameters were: a quadrate beam with size of  $\sim 35\mu\text{m} \times 25\mu\text{m}$ , the laser fluence  $\sim 4\text{J}/\text{cm}^2$ ; scanning velocity  $0.15\text{mm}/\text{min}$ , pulse repetition rate  $12\text{Hz}$ . Fig. 10(b) is a special shaped channel ablated into a SMF-28 fiber. Laser scanning was performed along a path as line 1 to 2, and so on. Laser spot is about  $10\mu\text{m} \times 10\mu\text{m}$ , and scanning velocity is  $0.12\text{mm}/\text{min}$ . on the whole, the micromachining quality of those microstructures is considerably good.



(a)



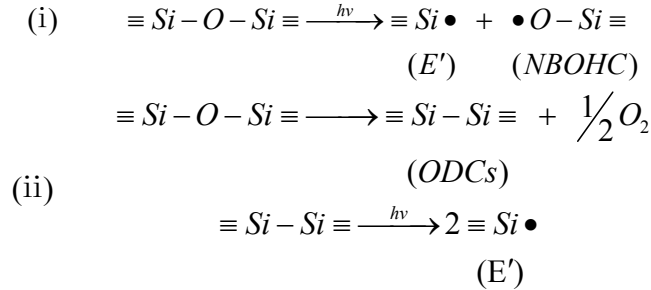
(b)

Fig.10. The NC process tool-path and ablated images of 157nm laser micro-fabrication (a) on a silica chip (b) on a silica fiber

#### 4. Discussion

Fused silica has a  $\sim 9.3\text{eV}$  bandgap energy, equivalent to  $133\text{nm}$  wavelength. Practical lasers are not yet available at the bandgap energy ( $9.3\text{eV}$ ). At  $157\text{nm}$  wavelength, fused silica is only weakly absorbing,  $\alpha = 10\text{cm}^{-1}$ <sup>[10]</sup>, but from our experiments and literature<sup>[10,11,13,14,15]</sup>, the  $157\text{nm}$  lasers nevertheless provide sufficiently strong interaction that smooth etched surfaces can be precisely excised, free of micro-cracks and with little debris. The inverse of the slope provides an effective single-photon absorption coefficient of  $\alpha_{\text{eff}} = 170,000\text{cm}^{-1}$  — a 17,000-fold

increase that attests to the importance of defect formation during such single-pulse interactions. This is due to, the 157nm output of the F<sub>2</sub> laser, which strongly couples energy into glass via defects, dopants or near-bandedge states, provides one approach for micromachining glass. In general, germanium and other elements are doped into silica fibers or glasses. Fused silica has ~8-eV bandgap energy, and bonding energy of Si-O is 4.5eV<sup>[10]</sup>. The dopants lower the bandgap and provide copious new defect centers. And then, induced by irradiation of 157nm laser, many defects such as NBOHCs, ODCs and E' centers were also created. The possible processes for photoinduced defect formation in the fused silica upon F<sub>2</sub> laser irradiation can be given by:



The photoexcited states of Si-O-Si rings would result in dissociation into pairs of NBOHCs and E' centers [process (i)] or formation of ODCs accompanied by interstitial oxygen molecules [process (ii)]. The photoinduced ODC defects were also excited by F<sub>2</sub> laser, which led to the formation of E' centers. All of them would cause the ablation threshold was lowered, sometimes to 70%. Due to the large photon energy of 7.9-eV, it is easy to break the bonding of silica glasses for 157nm laser, only by one-photon-absorption processes. In fact, when fused silica exposed to 157nm laser irradiation, ion (Si<sup>+</sup>, O<sup>+</sup>) emission phenomenon and changes of ion intensities have been observed<sup>[16]</sup>. That is also evidence of photo-chemical interaction.

Unlike material removal by 193nm and 248nm excimer laser, which are mainly by photo-thermal effect<sup>[17]</sup>, few of heat generated during ablation of 157nm laser<sup>[18,19]</sup>. However, there is still evidence of weak thermal effect in 157nm laser ablation. For example, slight color-difference resulted from heat on glass surface can be observed, as shown in Fig. 6 and Fig. 10. After all, the 157nm laser ablation is one-photon-absorption process for silica glasses or fibers, accompanying with weak thermal effect only.

## 5. Conclusions

A new micro-manufacturing tool -157nm DUV laser is demonstrated in this paper. For 157nm laser ablation of fused silica, the material removal is predominantly photo-chemical reaction induced by one-photon absorption process. Experiments and analysis show that: (1) the ablation rate of fused silica is about 75nm/pulse under laser fluence of ~4J/cm<sup>2</sup> and spot size smaller than 35μm. But when the number of pulses increases, the ablation rate would drop down gradually. (2) Take into account the machining efficiency, a better ablation quality can be achieved under the repetition rate of ~10Hz. (3) 157nm DUV laser processing has great potential for precision microfabrication of hard materials for practical applications.

## Acknowledgements

This work was financially supported by the National Natural Science Foundation of China (Grant No.50775169 and No.60537050).

## References

- [1] M. Edward Motamedi, Ming C.Wu and Kristofer S.J.Pister.  
Micro-opto-electro-mechanical devices and on-chip optical processing. Opt. Eng., Vol.

- 36 (1997) 1282-1297.
- [2] W. Zhang and J. Xiong. Micro-Optical-Electro- Mechanical-System, MOEMS. China Machine Press, (2006).
  - [3] Ming C. Wu. Micromachining for Optical and Optoelectronic Systems. Vol.85, No.11(1997) 18333-1856.
  - [4] Fei-fan Chen, Ling Yin and Yun-long Li. Review and Prospects of Research on Micro-opto-electro- mechanical System. Microfabrication Technology. No.3(2002) 1-7.
  - [5] Hiroaki Misawa and Saulius Juodkazis. 3D Laser Microfabrication. Wiley-VCH Verlag GmbH&Co.KgaA, (2006).
  - [6] J.F. Li, Microfabrication Technology of Three- Dimensional Microdevices and Their MEMS Application. Inorganic Materials, 17(4) (2003) 657-664.
  - [7] Ivan Fanderilik. Silica Glass and its Application. Amsterdam: ELSEVIER(1991).
  - [8] Levy D.H. and Gleason K.K. Reactions of Hydrogenated Defects in Fuled Silica Caused by Thermal Treament and Deep Ultraviolet Irradiation. Appl.Phys.Lett.,60(14)(1992) 1667-1669.
  - [9] Y. Wang and L. Liu. Silica Glass. Chemical Industry Press, (2006).
  - [10] P.R. Herman, R.S. Marjoribanks, et al. Laser Shaping of Photonic Materials: Deep-ultraviolet and Ultrafast Lasers. Applied Surface Science, 154-155(8)(2000)577-586.
  - [11] Y. Dai, D. Jiang and G. Xu. Micro- structuring of Photonic Materials by Deep-ultraviolet Laser. Proceedings of SPIE, 7284(2009)72840P1-6.
  - [12] Ryoichi Kuwano, Tsuyoshi Tokunaga, Yukitoshi Otani and Norihiro Umeda. Beam Shaping Optics for YAG Laser Processing Fabricated by Computerized Numerical Control Lathe. Optical Review Vol. 12, No. 6 (2005) 476-479.
  - [13] H. Deng, Y. Rao, Z. Ran, X. Liao, W. Liu. Photonic Crystal Fiber Based Fabry-Perot Sensor Fabricated by using 157nm Laser Micromachining. Acta Optica Sinica. 28(2)(2008)255-258.
  - [14] Y. Dai, W. Li and D. Jiang. Micro Ablation of Optical Fibers using Vacuum Ultraviolet Laser. Proc. Int. Conf. Integr. Commer. Micro Nanosyst, Sanya China. (2007)1353-1356.
  - [15] J. Greuters and N.H. Rizvi. Laser Micromachining of Optical Materials with a 157-nm Fluorine Laser, Proc. SPIE, Belgium, 4941(2003) 77-83.
  - [16] S.R. John, J.A. Leraas, S.C. Langford and J.T. Dickinson. Laser Induced Ion Emission from Wide Bandgap Materials. Applied Surface Science. 253(2007) 6283-6288.
  - [17] Y. Liao, Y. Chen, C. Chao and Y. Liu. Surface Morphology and Sub-surface Damaged Layer of Various Glasses Machined by 193nm ArF Excimer Laser. Proceedings of SPIE, 5717(2005)110-117.
  - [18] A. Pusel, P. Hess, et al. Photochemical Processing (157nm) of Semiconductor Surfaces without Heating. Surface Science, 74(11)(1999)433-435.
  - [19] Vaidynathan A, Walker T, et al. Comparison of Keldysh and Perturbation Formulas for One-photon Absorption. J. Physics Review, 20B(5)(1979)3526-3527.